

## SMART COMPOSITE MATERIAL MICROPHONE USING A GRATING FIBER OPTIC SENSOR

Madalin Ion RUSU<sup>1</sup>, Dan SAVASTRU<sup>2</sup>, Valeriu SAVU<sup>3</sup>, Alexandru STANCIU<sup>4</sup>,  
Marina TAUTAN<sup>5\*</sup>

*Simulation results on operation of a smart laminate polymer composite material use as a microphone sensitive element are presented. The main investigated grating optic fiber sensor was the Long Period Grating Fiber Sensor (LPGFS) with Long Period diffraction Grating (LPG), manufactured in standard communication Single Mode (SM) optic fiber. The LPGFS simulation process aims to define its characteristics as the feedback loop of an automatized smart laminate polymer composite material operated by observing acoustic energy effects on the system were also investigated the functional limits of a smart polymer laminate composite material imposed by delamination of the composite.*

**Keywords:** composite material; grating fiber optic; microphone sensor.

### 1. Introduction

There is an increased industrial need for fiber optic based acoustic detection is constantly increasing [1-6]. Industrial sectors, such as the oil industry, chemical industry, medical and special applications require the measurement of seismic waves using a more cost-effective approach to replace large arrays of all-electronic based geophones or hydrophones which are currently being used with high sensitivity optic fibers, but coupled with high cost and high fragility [1-8]. The optical fiber based acoustic sensors have demonstrated high versatility, low cost, high immunity to disturbance especially electromagnetic fields, therefore have shown promise for achieving the mentioned objectives. The main scope of the paper consists of presenting the results obtained analyzing the use of grating fiber optic sensor computation and simulation in optimization of Long Period Grating Fiber Sensor (LPGFS) embedded in polymer matrix of a composite material as microphone sensing element. Polymer composite materials are used as microphone sensing element fulfilling the industry needs for various applications [1-6]. A composite material is transformed into a smart one by embedding an optical fiber

<sup>1</sup> Eng., National Institute of R&D for Optoelectronics INOE 2000, Romania, e-mail: madalin@inoe.ro

<sup>2</sup> Eng., National Institute of R&D for Optoelectronics INOE 2000, Romania, e-mail: dsavas@inoe.ro

<sup>3</sup> Eng., National Institute of R&D for Optoelectronics INOE 2000, Romania, e-mail: savuv@inoe.ro

<sup>4</sup> Eng., National Institute of R&D for Optoelectronics INOE 2000, Romania, e-mail: alexandru.stanciu@inoe.ro

<sup>5\*</sup> Corresponding author - Eng., National Institute of R&D for Optoelectronics INOE 2000, Romania, e-mail: marina@inoe.ro

grating sensor into its polymer matrix. System simulations were performed to optimize a smart polymer composite material as microphone sensing element. Operational limits imposed by delamination or the separation of layers were identified as a common failure mode in laminated composite materials under applied vibration effects [7-16].

## 2. Theory

One development of optical fibers applications is based on sound-induced change of refractive index ( $n_{amb}$ ) of optic fiber ambient medium causing a shift in the frequency of the optical signal guided propagating through the core of a single mode (SM) optic fiber. Fiber optics are used for the detection of sound waves transmitted in different media. The interest is focused on LPGFS embedded into polymer matrix of laminate composite material plate which is used in a way similar to that of an old microphone membrane. The investigated system consists of a 20×60mm laminate polymer composite plates investigated as microphone sensing element [12-14]. The investigated polymer composite plate was made of three layers of 0.5 mm thickness with different relative orientations (90/45/0) with the LPGFS embedded into a central position of the plate between first and second layer [15-20]. The polymer matrix of the composite material was considered to be manufactured of polyvinyl-chloride (PVC) or Polydimethylsiloxane (PDMS) [21]. The polymer matrix is made of a material having a refractive index lower than that of fused silica – the material of the single mode optic fiber. It is assumed that the three layers are perfectly bonded together.

The investigated system of SCPM used as microphone sensing element are manufactured of LPGFS embedded into polymer matrix. A LPGFS consists of a single mode (SM) optical fiber basically used as light propagation guide into and from sensing zone and which is processed by inscribing a diffraction Bragg grating into it. Basically, LPGFS consists of a uniform or a modulated magnitude variation fiber core refraction index along it over a length of 5 - 75 mm with a period of 1 – 1000  $\mu$ m, defined as Long Period Grating (LPG). One important feature of the LPG is that the grating zone of the host optical fiber is placed in direct contact with the ambient and can be directly affected by the microscale possible changes of ambient measured by refractive index variations. In the investigated case, these microscale possible changes of ambient measured by refractive index variations are induced by the vibrations applied on SCPM [10-20, 22-32]. The LPGFS operation relies on observing the spectral broadenings and shifts of the absorption bands induced by the Bragg grating scattering in the optical fiber transmission spectrum. The absorption bands are induced by the coupling process between the fundamental mode propagating through the optical fiber core and the modes propagating through

the fiber cladding. The peaks of the absorption bands correspond to the Bragg resonance wavelengths of the LPG [10-20, 22, 33-35].

The LPGFS main part is the LPG. The modulation of the LPG is obtained by either inducing a physical deformation in the SM optical fiber material or by modifying the refractive index of the optical fiber core [16-20, 22, 33-35]. The latter is the more expensive standard method and the LPG is usually formed in photosensitive optical fiber core by creating color-center point defects induced by exposing the core material to ultraviolet (UV) laser light - typically in the 242 nm to 248 nm wavelength range [16-20]. A main drawback of the LPG manufactured using this technology is that the color-centers are thermally unstable from temperatures greater than 250-300°C [22-25, 33-35]. The physical deformation in the fiber material is the cheaper fabrication technique which becomes more and more popular. This technique is accomplished by thermal processing of the optical fiber using CO<sub>2</sub> laser point-by-point illumination or by electric arc discharge applied repetitively [26-29]. The physical deformation basically consists in forming periodic slight tapers of the SM optical fiber. Compared to other optical devices, LPGs have several advantages such as the simple fabrication techniques, they are small volume intrinsic optical fiber devices and their non-conducting (dielectric) structure is immune to electromagnetic interference [16-20, 22-25, 33-35]. LPGFS have low-level back reflection and low insertion losses, as well as being relatively insensitive to polarization effects when fabricated using UV laser radiation [16-20, 22-25, 33-35].

The LPGFS operation is described by the Eq. (1):

$$\lambda^{(i)} = \left( n_{eff}(\lambda^{(i)}) - n_{clad}^{(i)}(\lambda^{(i)}) \right) \Lambda$$

where  $n_{eff}(\lambda^{(i)})$  is the effective value of the core refraction index and  $n_{clad}^{(i)}(\lambda^{(i)})$  is the refractive index effective value of the cladding corresponding to  $\lambda^{(i)}$  the light propagating through the optic fiber core and to the possible light cladding co-propagating modes. For each  $\lambda^{(i)}$  the coupling coefficient between the core and the  $i^{\text{th}}$  cladding mode,  $\kappa_i$ , is calculated using Bragg resonance wavelength value, the grating modulation period and amplitude values [16-20, 22-25, 33-35]. From Eq. (1), the grating characteristic Phase Matching Curves (PMC) are calculated. PMC are parametric curves defining the pairs grating period  $\Lambda$  and Bragg resonance wavelength values  $\lambda^{(i)}$ . In Eq. (1)  $n_{eff}$  and  $n_{clad}^{(i)}$  are both functions of the investigated system mechanical status which is dependent on applied vibrations equivalent to twisting and/or bending the SCPM. Finally, the SCPM twisting and/or bending means strain created in the system which is equivalent to spectral shifts of the LPG absorption peaks and broadening of the corresponding bands.

In Figure 1 there is schematically represented a virtually setup, easy convertible into an experimental one, which allows studies on an LPG operation as a sound detector [11,12]. The idea of the setup presented in Figure 1 is that

vibrations propagating into a continuum medium are equivalent to compression/elongation, bending, opening, shearing or tearing strain induced into elemental volume elements of the medium. For the work presented in the article, one main issue consists of analyzing the LPG response at such applied stresses [11,12].

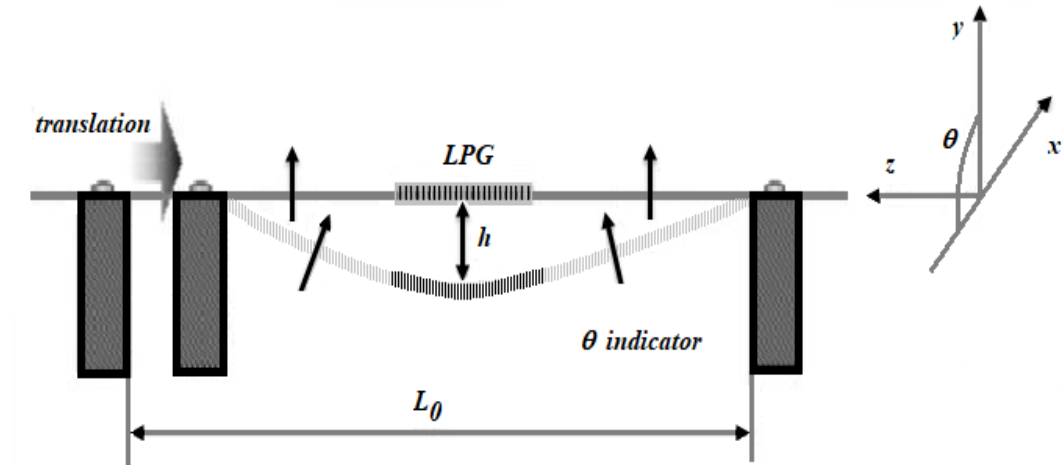


Fig. 1. Schematics of a LPGFS sounds detector.

### 3. Simulation Results

The LPGFS of the SCPM microphone system was investigated in three stages. The simulations were accomplished considering a grating with a length of 50 mm, an amplitude of core refraction index modulation amplitude  $\delta n_\infty$  of  $2 \times 10^{-4}$  and a visibility of 1. During simulations it was considered that the investigated LPGFS is embedded in the PDMS matrix of a composite material. During simulations the PDMS/PLA refractive index was 1.4303. In the first stage  $n_{\text{eff}}$  and are calculated. In Fig. 1 are presented the LPGFS dispersion curves, i.e., the variations versus wavelength of core fundamental mode and first 9 modes propagating through the cladding. The Calculated values are introduced into Eq. 1 for the stage of simulation.

In Figure 2 there are presented the core and cladding effective refractive index values versus light wavelength simulated in the case of a LPGFS embedded in PDMS.

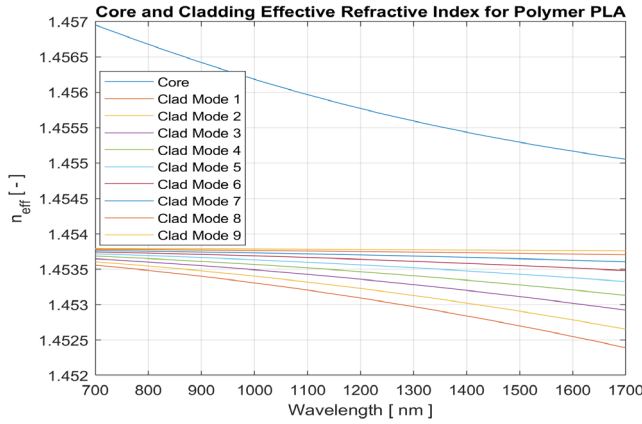


Fig. 2. Core and Cladding Effective Refractive Index Values vs Wavelength simulated for LPGFS embedded in PDMS.

In Fig. 3 the results obtained in the second simulation stage, namely the Phase Matching Curves (PMC), are presented. The PMC of the investigated LPGFS is represented in a coordinate system (wavelength - LPG period, denoted as  $\Lambda_{LPG}$ ). In Figure 3 it can be noticed that a line corresponding to  $\Lambda_{LPG}$  of 775  $\mu\text{m}$  and parallel to wavelength axis intersects the PMC in 7 points corresponding to Modes 1 to 7. These intersection points correspond each to a  $\lambda^{(i)}$  value. There are kept only the first seven Modes because higher ones correspond to  $\lambda^{(i)}$  situated outside the spectral range of interest. Because of a higher accuracy, the simulations were accomplished using an analytical method of  $\lambda^{(i)}$  calculation not a graphical one.

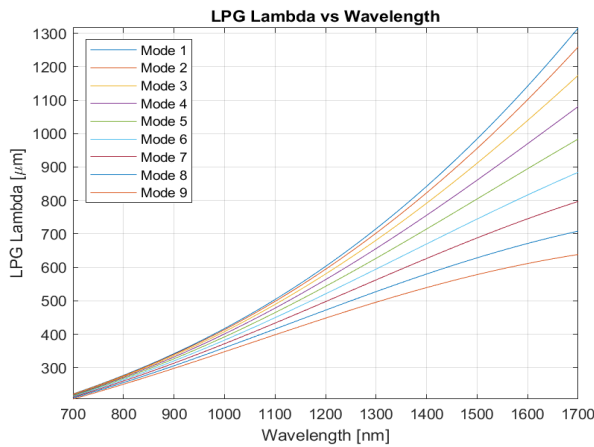


Fig. 3. Phase Matching Curves obtained for LPGFS embedded in PDMS.

In Fig. 4 the results obtained in the next simulation stage, namely the LPGFS transmission spectrum for a 775  $\mu\text{m}$  grating period are presented. In Fig. 4 it can be observed that the absorption Bragg resonance bands have decreasing

intensities corresponding to inverse modes order. This is caused because the mode denomination used in the computer simulation algorithm. In Figure 4 the modes having longer resonance wavelength are the ones for which the Bragg resonance condition is easier accomplished. These are the cladding modes which propagate closer to the optic fiber axis.

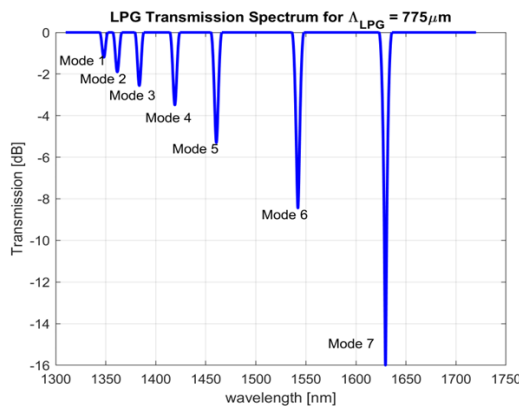


Fig. 4. The simulated transmission spectrum of the investigated LPGFS.

As observed in transmission spectrum LPGFS, each mode has spectroscopic characteristics such as bandwidth and strength/amplitude. In Figure 5 there is presented the simulated transmission spectrum of such mode, namely Mode 6. It can be observed that Mode 6 has a Full Width Half-Measure (FWHM) of 4.25 nm and an amplitude of -9.48 dB in decibels.

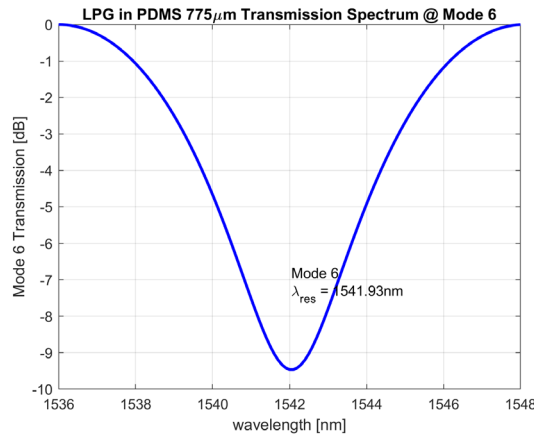


Fig. 5. This is a figure. Schemes follow the same formatting.

In Figure 6 there is presented the spectral shift variation of Mode 6 Bragg resonance wavelength versus ambient refractive index. The spectral shift variation of Mode 6 Bragg resonance wavelength is calculated versus the situation of the LPGFS placed in air with no mechanical stress applied.

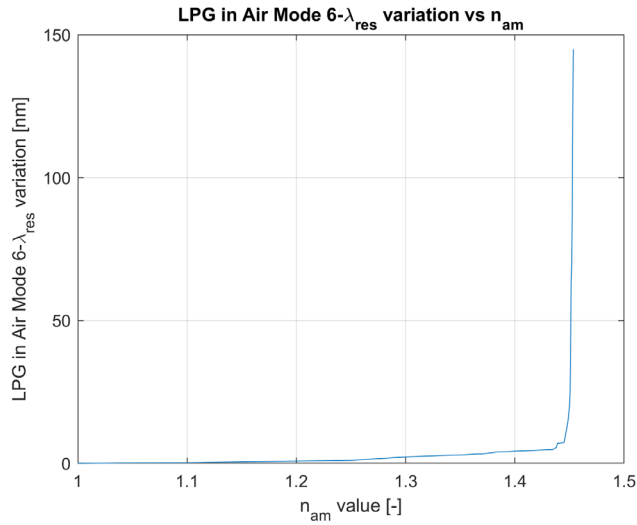


Fig. 6. Spectral shift variation of Mode 6 Bragg resonance wavelength vs ambient refractive index.

In Fig. 6 there are presented the results simulated when an external bending mechanical load is applied on LPGFS. In Figure 1 the external bending mechanical load is applied along an axis z perpendicular to the composite plate, in the +z direction, from the composite plate surface. At different strains induced in the optical fiber by the external bending mechanical load applied on the investigated composite plate Mode 6 resonance wavelength suffers a spectral shift as in the Fig. 6. A quite linear spectral shift for the induced strain can be noticed, enabling an accurate determination of the strain. In Fig. 8 there are presented the three analyzed cases when an external twisting mechanical load is applied. In Figure 1, the external twisting mechanical load is applied along an axis z perpendicular to the composite plate, in the -z direction, towards the composite plate surface in one point and in the +z direction in the second point. A unit external mechanical load is considered. At different strains induced in the optical fiber by the external twisting mechanical load applied on the composite plate Mode 6 resonance wavelength suffers a spectral shift as in the Fig. 7. In the figure there is plotted the variation of Mode 6 resonance wavelength spectral shift vs induced strain in the case of two semi-circular load application zones.

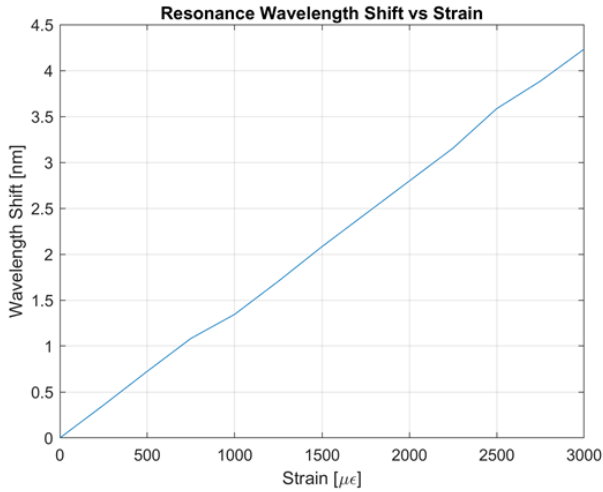


Fig. 7. The simulated Mode 6 resonance wavelength spectral shift versus strain induced by bending mechanical load.

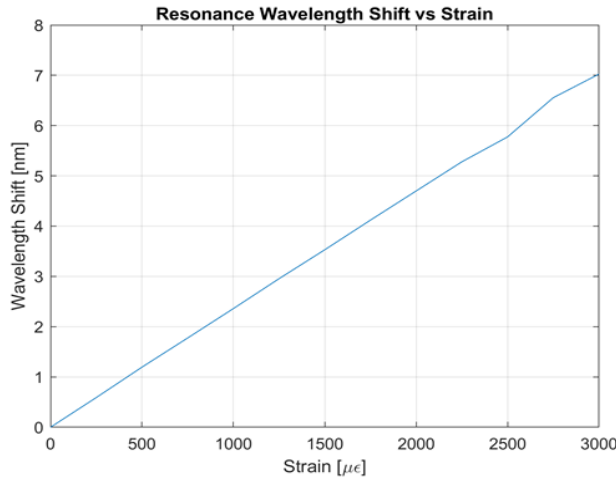


Fig. 8. The simulated Mode 6 resonance wavelength spectral shift versus strain induced by twisting mechanical load.

At different strains induced in the optical fiber by the external twisting mechanical load applied on the composite plate Mode 6 resonance wavelength suffers a spectral shift as in the Fig. 8. In the figure there is plotted the variation of Mode 6 resonance wavelength spectral shift vs induced strain in the case of two semi-circular load application zones. The Mode 6 resonance wavelength spectral shift values are up to 20 % larger than those obtained in the same case for the bending load. A quite linear spectral shift for the induced strain can be noticed, enabling an accurate determination of the strain.

#### 4. Discussion

For the authors the presented results are the very first stage of a study concerning the implementation of grating fiber sensors in various medical, research, industrial and special application fields. This first stage consists mainly in creating the software packages of codes covering possible applications. Future research directions resulting from the mentioned study will be reported when and together with obtained experimental results.

#### 5. Conclusions

A finite element method analysis of possible application of smart composite materials based on an optical fiber grating sensor embedded in the polymer matrix of the smart composite material used as microphone operated in vibration fields was developed. These smart composite materials are intended to be used in mechanical structures and parts construction of industrial installations. The composite material is transformed into a smart one by using the optical fiber grating sensor signal as input into a feedback loop of an automatization system. Analysis of the LPGFS embedded into the PDMS polymer matrix of a SPCM response with applied bending or twisting mechanical loads is accomplished using a self-developed simulation model. The simulation model considers a simple LPGFS setup one. The main purpose of developed simulation model consists into development of a software toolbox dedicated to improved design of SPCM applications. The simulation results are obtained using a self-made software set developed based on a commercial software package (MATLAB 9.2). There were observed a good agreement between the simulation and experimental results. On one hand, the developed simulation model is useful for discerning between the effects of SPCM response to externally applied mechanical loads from the environment. On the other hand, the developed simulation model is intended to improve the SPCM manufacturing tailored to specific applications, mainly in aeronautics and chemical industry. Further developments will be accomplished concerning the non-linear effects due to long period grating itself and/or induced by its manufacturing technology.

The developed LPGFS simulation model will allow improved design of smart composite materials with various applications in chemical industry including their operation as chemical sensors. Smart composite materials using optical fiber sensors, particularly LPGFS, represent a relative new domain of applicative research.

#### Acknowledgements

This work was supported by the Core Program within the National Research Development and Innovation Plan 2022-2027, carried out with the support of

MCID, project no. PN 23 05, the Romanian Ministry of Research, Innovation and Digitalization, and a grant of the Ministry of Research, Innovation and digitalization, CNSC-UEFISCDI, project number PN-III-P4-PCE-2021-0585, within PNCDI III.

## REFERENCES

- [1]. Aleksey Mironov, Andrejs Kovalovs, Andris Chate and Aleksejs Safonovs S. Author, T. More. “Static Loads Influence on Modal Properties of the Composite Cylindrical Shells with Integrated Sensor Network”, Sensors, **vol. 23**, no. 6, 2023, pp. 3327,
- [2]. Yu Zhang, Yu Feng, Xiaobo Rui, Lixin Xu, Lei Qi, Zi Yang, Cong Hu, Peng Liu and Haijiang Zhang, “Acoustic Source Localization in CFRP Composite Plate Based on Wave Velocity-Direction Function Fitting” Sensors, **vol. 23**, no. 6, 3052, 2023. DOI: 10.3390/s23063052
- [3]. B. Degamber, G.F. Fernando, “Process Monitoring of Fiber-Reinforced Polymer Composites”, MRS Bulletin, **vol. 27**, no. 5, 2002, pp. 370-380.
- [4]. K. Bocz, D. Simon, T. Bárány, G. Marosi, “Key Role of Reinforcing Structures in the Flame-Retardant Performance of Self-Reinforced Polypropylene Composites”, Polymers. **vol. 8**, 2016, pp. 289-301.
- [5]. K. Dobrovszky, F. Ronkay, “Effects of Phase Inversion on Molding Shrinkage, Mechanical, and Burning Properties of Injection-molded PET/HDPE and PS/HDPE Polymer Blends”, Polymer-Plastics Technology and Engineering, **vol. 56**, no.11, 2017, pp. 1147-1157.
- [6]. N. Malhotra, M. Kundabala, S. Acharya, “Strategies to Overcome Polymerization Shrinkage - Materials and Techniques, A Review”, Dental update, **vol. 37**, no. 2, 2010.
- [7]. J.K. Lee, J.K. Gillham, “Evolution of properties with increasing cure of a thermosetting epoxy/aromatic amine system: physical ageing”, J Appl Polym Sci, **vol. 90**, no.10, 2003, pp. 2665-2675.
- [8]. M.A. El-Sherif and J. Radhakrishnan, “Advanced Composites with Embedded Fiber Optic Sensors for Smart Applications”, Journal of reinforced Plastic and Composites, **vol.16**, no.2, 1997
- [9]. J.H.L. Grave, M.L. Håheim, A.T. Echtermeyer. “Measuring changing strain fields in composites with Distributed Fiber-Optic Sensing using the optical backscatter reflectometer”, Composites Part B, **vol. 74**, 2015, pp. 138-146.
- [10]. S.W. James, R.P. Tatam, “Optical fibre long-period grating sensors: characteristics and application”, Meas Sci Technol, **vol. 14**, no. 5, 2003, R49–R61.
- [11]. A.M. Vengsarkar, P.J. Lemaire, J.B. Judkins, V. Bhatia, T. Erdogan, J.E. Sipe, “Long-period fibre gratings as band-rejection filters”, J Lightwave Technol, **vol. 14**, no. 1, 1996, pp. 58–65.
- [12]. T. Erdogan, “Cladding-mode resonances in short- and long- period fiber grating filters”, J Opt Soc Am A, **vol. 14**, no. 8, 1997, pp. 1760–1773.
- [13]. T. Erdogan, “Fiber grating spectra”, J Lightwave Technol, **vol. 15**, no. 8, 1997, pp. 1277–1294.
- [14]. A.I. Kalachev, V. Pureur, D.N. Nikogosyan, “Investigation of long-period fiber gratings induced by high-intensity femtosecond UV laser pulses”, Opt Commun, **vol. 246**, no. 1-3, 2005, pp. 107–115.
- [15]. C.S. Cheung, S.M. Topliss, S.W. James, R.P. Tatam, “Response of fibre optic long period gratings operating near the phase matching turning point to the deposition of nanostructured coatings”, J Opt Soc Am B, **vol. 25**, no. 6, 2008, pp. 897–902.

- [16]. *L. Zhang, W. Zhang, I. Bennion*, “In-Fiber Grating Optic Sensors” In: S. Yin, P.B. Ruffin, F.T.S. Yu editors, *Fiber Optic Sensors*. Second Edition. Boca Raton, FL: CRC Press, 2008, pp. 109–162.
- [17]. *W.J. Bock, J. Chen, P. Mikulic, T. Eftimov*, “A novel fiber-optic tapered long-period grating sensor for pressure monitoring”, *IEEE T Instrum Meas*, **vol. 56**, no. 4, 2007, pp. 1176–1180.
- [18]. *D. Savastru, S. Miclos, R. Savastru, I. Lancranjan*, “Numerical analysis of a smart composite material mechanical component using an embedded long period grating fiber sensor”, *Proc SPIE Int Soc Opt Eng*, 2015, **vol. 9517**, art. no:95172A. DOI: 10.1117/12.2188231.
- [19]. *S. Miclos, D. Savastru, R. Savastru, I. Lancranjan*, “Numerical analysis of Long Period Grating Fibre Sensor operational characteristics as embedded in polymer”, *Compos Struct*, **vol. 183**, 2018, pp. 521-526, doi: <http://dx.doi.org/10.1016/j.compstruct.2017.04.079>, IDS No: FL9QV
- [20]. *D. Savastru, S. Miclos, R. Savastru, I. Lancranjan*, “Study of thermo-mechanical characteristics of polymer composite materials with embedded optical fibre”, *Compos Struct*, **vol. 183**, 2018, pp. 682-687.
- [21]. *A. Groza, A. Surmeian, C. Diplasu, P. Chapon, D. Manaila-Maximean and M. Ganciu*, “GD-OES and GD-MS investigations of the processes involved in the polymerization of polydimethylsiloxane in corona discharges” *University Politehnica of Bucharest Scientific Bulletin-Series A-Applied Mathematics and Physics*, **vol. 73**, no.3, 2011, pp.133-140.
- [22]. *V. Bhatia, D.K. Campbell, D. Sherr, T.G. D'Alberto, N.A. Zabaronick, G.A. Ten Eyck, K.A. Murphy, R.O. Claus*, “Temperature-insensitive and strain-insensitive long-period grating sensors for smart structures”, *Optical Engineering*, **vol. 36**, no. 7, 1997, pp. 1872-1875.
- [23]. *K.O. Hill, B. Malo, F. Bilodeau, D.C. Johnson*, “Photosensitivity in optical fibers”, *Annu Rev Mater Sci*, **vol. 23**, 1993, pp. 125–157.
- [24]. *R. Falciai, A.G. Mignani, A. Vannini*, “Long period gratings as solution concentration sensors”, *Sensor Actuat B-Chem*, **vol. 74**, no. 1-3, 2001, pp. 74–77.
- [25]. *S. Korposh, R. Selyanchyn, W. Yasukochi, S.W. Lee, S.W. James, R.P. Tatam*, “Optical fiber long period grating with a nanoporous coating formed from silica nanoparticles for ammonia sensing in water”, *Mater Chem Phys*, **vol. 133**, no. 2-3, 2012, pp. 784–792.
- [26]. *X. Shu, D. Huang*, “Highly sensitive chemical sensor based on the measurement of the separation of dual resonant peaks in a 100-m-period fiber grating”, *Opt Commun*, **vol. 171**, no. 1-3, 1999, pp. 65–69.
- [27]. *B. Malo, S. Theriault, D.C. Johnson, et al.* “Apodised in-fiber Bragg grating reflectors photo-imprinted using a phase mask”, *Electron Lett*, **vol. 31**, no. 3, 1995, pp. 223–225.
- [28]. *X.L. Li, W.G. Zhang, J. Ruan, S.S. Zhang*, Temperature- and strain-insensitive torsion sensor based on phase shifted ultra-long-period-grating. *Electron Lett*, **vol. 48**, no. 4, 2012, pp. 235–236.
- [29]. *L.A. Everall, R.W. Fallon, J.A.R. Williams, L. Zhang, I. Bennion*, Flexible fabrication of long-period in-fiber gratings, *Proceedings of Conference on Lasers and Electro-Optics CLEO '98*, San Francisco, California, 1998, pp. 513–514.
- [30]. *B. Li, L. Jiang, S. Wang, H.L. Tsai, H. Xiao*, Femto-second laser fabrication of long period fiber gratings and applications in refractive index sensing, *Opt Laser Technol*, **vol. 43**, no. 8, 2011, pp. 1420–1423.
- [31]. *I. Lancranjan, D. Savastru, S. Miclos, A. Popescu*, “Numerical simulation of a DFB-fiber laser sensor (II) – theoretical analysis of an acoustic sensor”, *J. Optoelectron. Adv. Mater.* **vol. 12**, no. 12, 2010, pp.2456–2461, IDS No.704HW
- [32]. *S. Miclos, D. Savastru, I. Lancranjan*, “Numerical simulation of a fiber laser bending sensitivity”, *Rom. Rep. Phys.*, **vol.62**, no.3, 2010, pp.519-527, IDS No.720HU

- [33] *D. Savastru, S. Miclos, R. Savastru, I.I. Lancranjan*, “Analysis of mechanical vibrations applied on a LPGFS smart composite polymer material”, *Compos Struct*, **vol. 226**, art. no. 111243, 2019, pp. 1243-1250.
- [34]. *S. Miclos, D. Savastru, R. Savastru, I.I. Lancranjan*, “Transverse mechanical stress and optical birefringence induced into single-mode optical fibre embedded in a smart polymer composite material”, *Compos Struct*, **vol. 218**, 2019, pp. 15-26.
- [35]. *E. Anemogiannis, E.N. Glytsis, T.K. Gaylord*, “Transmission characteristics of long period fiber gratings having arbitrary azimuthal/radial refractive index variations”, *J Lightwave Technol*, **vol. 21**, no. 1, 2003, pp. 218–227.